EMG-based Position and Force Control of a Robot Arm: Application to Teleoperation and Orthosis

Panagiotis K. Artemiadis Kostas J. Kyriakopoulos
Control Systems Lab, School of Mechanical Eng.
National Technical University of Athens,
9 Heroon Polytechniou Str, Athens, 157 80, Greece
{*partem,kkyria*}*@mail.ntua.gr*

***Abstract*— This paper presents a methodology for the control of a robot arm, using electromyographic (EMG) signals. EMG signals from the muscles of the shoulder and elbow joints are used to predict the corresponding joint angles and the force exerted by the user to the environment through his/her forearm. The user's motion is restricted to a plane. An analysis of various parametric models is carried out in order to define the appropriate form of the model to be used for the EMG-based estimates of the motion and force exerted by the user. A multi-input multi-output (MIMO) black-box state-space model is found to be the most accurate and is used to predict the joint angles and the force exerted during motion, in high frequency. A position tracking system is used to track the shoulder and elbow joint angles in low frequency to avoid drifting phenomena in the joints estimates. The high frequency model estimates, the low-frequency position tracker and a Kalman filter are used to control a torque controlled robot arm in the frequency of 500 Hz. The proposed system is tested both on teleoperation and orthosis scenarios. The experimental results prove the high accuracy of the system within a variety of motion profiles.**

***Index Terms*— EMG-based control, teleoperation, orthosis**

I. Introduction

As the ubiquity of robots has become evident, the issue of human-robot interface has received increased attention. When the issue of interface comes to the level of control, conventional algorithms are replaced by intelligent systems and decision methods. For this reason, there is an increasing demand for a direct and more natural means of interface between the user and the controlled robot. A possible approach is the use of electromyographic (EMG) signals from skeletal muscles, because of their advantage of being both convenient and natural for the master. Since muscles are responsible not only for moving the human limbs but also for exerting forces to the environment, EMG signals can be proved useful for the control of a robot arm, especially in the cases where the arm is controlled in position and force.

Telerobotics is an area that can be mostly benefitted by the use of the electromyogram, by using it as the human-robot interface. Fukuda [1] firstly introduced the idea of teleoperation of a robot arm using EMG signals and a position tracking system. Wrist movement was extracted from EMG signals from the forearm muscles, while a position tracker was used to teleoperate the lower arm of the robot. The authors have also used in the past EMG signals to control a robot arm in planar reaching tasks in [2].

Concerning orthotic devices, a lot of robotic mechanisms intended for either rehabilitation or extension of human ability have been developed during the last decades. As examples of the latter, Kazerooni proposed a new class of robot manipulators worn by humans in [3]. Similar orthotic devices for the upper limb have been developed and presented in [4], where EMG signals were used as the main control signal for the exoskeleton providing high intuitiveness.

A lot of different methodologies have been proposed for the utilization of EMG signals to control robots. A pattern classifier technique has been used for identifying finger motion based on EMG signals in order to drive a prosthetic hand in [5]. A Hill-based muscle model was used to estimate human joint torque in driving an exoskeleton in [4]. The authors have implemented an algorithm using an auto-regressive moving average with exogenous output (ARMAX) model, for estimating planar motion of the human arm during reaching, in order to teleoperate a robot arm [2]. However, there is limited literature on combined position and force estimation using EMG signals, which is undoubtedly a challenging issue for the control of a robotic device either is remotely teleoperated or coupled with the human arm.

In this paper, a methodology for controlling a robot using EMG signals from the muscles of the human upper limb is proposed and tested through real-time experiments. Surface EMG signals are recorded from muscles of the elbow and shoulder joints, while motion is restricted to a plane. A position tracking system is also used for monitoring the human arm motion, in the frequency of 60 Hz. EMG signals, recorded in the frequency of 1 kHz, are used to estimate both human motion and force exerted from the user to the environment in the same frequency. The high frequency motion estimates based on EMG signals are refined in real time using the low frequency measurements of the position tracking system, in order to avoid drifting phenomena, by applying a filtering technique. For the generation of the estimates, an analysis of various models is conducted. The motion and force estimated are used to control the robot arm. The system is tested using two scenarios: initially the arm is remotely operated by the user, while in the second setup, the human arm is firmly coupled with the robotic arm at its end-effector. The experimental results show that the efficiency of the EMG-based architecture is adequate for controlling the torque-controlled robot arm with high accuracy, within a variety of situations.

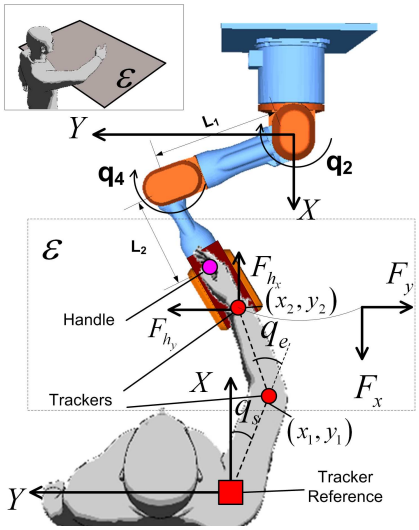

Fig. 1. User's plane of motion, joint angles, force exerted and reference axes. Position trackers 1, 2 are placed at points (x_1, y_1), (x_2, y_2) respectively, user exerts forces F_{h_x}, F_{h_y}, while robot exerts opposite forces F_x, F_y.

The rest of the paper is organized as follows: Section II gives a description of the methodology proposed, with the appropriate segregation of the sub-problems. Section III illustrates the efficiency of the approach through a number of experimental results, while section IV concludes the paper.

II. Methodology

In this section, the analysis and identification of the model relating EMG to motion and force will be discussed. Then, the application of the filtering technique using the position tracker measurements will be analyzed.

A. EMG-based Model Analysis and Identification

User's motion is restricted to a plane ε perpendicular to user's torso at the height of the shoulder, as shown in Fig. 1. Thus the motion in joint space was restricted to shoulder transverse adduction-abduction and elbow flexion-extension. The main responsible muscles for shoulder motion (i.e pectoralis major (clavicular head) and deltoid (lateral)) and for elbow motion (i.e. biceps brachii and triceps brachii) are recorded using single differential surface EMG electrodes (DE-2.1, Delsys Inc.) connected to an EMG system (Bagnoli-16, Delsys Inc.).The signals are pre-amplified with a gain factor of 1000 and acquired through a signal acquisition board (NI-DAQ 6036E) using sampling frequency of 1kHz. Then they are full-wave rectified, low-pass filtered (4^{th} order Butterworth filter) and normalized to their maximum voluntary isometric contraction value. The resulting form is used as input to the model to be estimated. Consequently the model has four inputs.

For the identification procedure, the model outputs should be defined and measured along with the input signals. The system has four outputs, consisting of elbow and shoulder joint angles and two components of force exerted from the user to the environment, as shown in Fig. 1. Measurement of joint angles is accomplished by using a position tracking system (Isotrak II, Polhemus Inc.). The tracker sensors are placed on the elbow and wrist of the user, while their reference system is placed on the shoulder of the user as shown in Fig. 1. The size of the position sensors is 2.83(W) 2.29(L) 1.51(H) cm.

The user's wrist joint is immobilized at zero position by means of straps on a support base equipped with a handle for the user's hand. The support base is mounted on the end-effector of a 7 degrees of freedom (DoFs) robotic manipulator (PA-10, Mitsubishi Heavy Industries), which is properly configured to support the user's hand against gravity. Two robotic joints are free to move, while the others are fixed through electromechanical brakes, in such configuration allowing the robotic arm to move on the same plane that the user's arm moves. The robot arm was controlled in such a way simulating a two-dimensional spring with variable stiffness. Thus, when the user moves his/her arm on the plane ε shown in Fig. 1, he/she has to exert force to the environment (robot arm) in order to deform the virtual two-dimensional spring. The spring is at its equilibrium point (zero force) when the robot arm is fully extended, while the stiffness at both directions is given by a 2^{nd} order polynomial function of the distance from equilibrium point at each axis of motion. A variable stiffness is used in order to achieve larger heterogeneity in exerted force profiles. Maximum values for the two components of force are defined in advance and correspond to maximum distance from equilibrium point at each direction. Considering the kinematic equations of the robot arm

$$\begin{aligned} X &= L_1 \cos(q_2) + L_2 \cos(q_2 + q_4) \\ Y &= L_1 \sin(q_2) + L_2 \sin(q_2 + q_4) \end{aligned} \tag{1}$$

where L_1, L_2 the link lengths and q_2, q_4 the moving joint angles, keeping the original numbering of the joint angles of the 7-DoF robot arm, the maximum distances X_{max}, Y_{max} from the equilibrium position along the x and y axes respectively, are given by $X_{\max} = Y_{\max} = L_1 + L_2$, and the equilibrium point coefficients (X_o, Y_o) are given from the kinematic equations (1) for $q_2 = q_4 = 0$ as shown below:

$$X_o = L_1 + L_2, \qquad Y_o = 0 \tag{2}$$

Thus if $F_{x(\max)}$, $F_{y(\max)}$ the maximum values for the x, y components of force, the two components of force exerted by the virtual spring are given by:

$$\begin{aligned} F_x^{(3)} &= 2\tfrac{F_{x(\max)}}{(L_1+L_2)^3}X^3 - 3\tfrac{F_{x(\max)}}{(L_1+L_2)^2}X^2 + F_{x(\max)} \\ F_y^{(3)} &= -2\tfrac{F_{y(\max)}}{(L_1+L_2)^3}Y^3 + 3\tfrac{F_{y(\max)}}{(L_1+L_2)^2}Y^2 \end{aligned} \tag{3}$$

where F_x, F_y the components of force along the x, y axes and X, Y the robot arm end-effector position given by (1). The graphical representation of the simulated two-dimensional spring that acts on the plane of user's motion is depicted in Fig. 2. In order the robot arm to exert the above mentioned force to the user through the handle mounted at the support base as shown in Fig. 1, the following torque command should be sent to the motors of the moving robotic joints:

$$\tau = \mathbf{I}\ddot{\mathbf{q}} + \mathbf{F_{fr}}(\dot{\mathbf{q}}) + \mathbf{J^T}(\mathbf{q})\,\mathbf{F} \tag{4}$$

where $\tau = \begin{bmatrix} \tau_2 & \tau_4 \end{bmatrix}^T$ the torque vector sent to the motors of the robot arm, $\mathbf{I}$ the 2×2 tensor of inertia of the two DoF arm, $\ddot{\mathbf{q}}$ the joint acceleration vector, $\mathbf{F_{fr}}$ the friction vector at

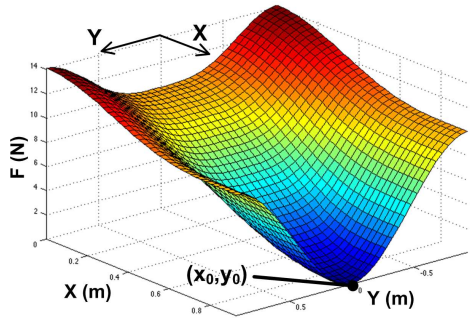

Fig. 2. Graphical representation of the simulated two-dimensional spring force along the robot workspace.

each joint, $\mathbf{F} = \begin{bmatrix} F_x & F_y \end{bmatrix}^T$ the vector of exerted force and $\mathbf{J}(\mathbf{q})$ the two DoF arm Jacobian matrix given by:

$$\mathbf{J} = \begin{bmatrix} L_1 c_2 + L_2 c_{24} & L_2 c_{24} \\ -L_1 s_2 - L_2 s_{24} & -L_2 s_{24} \end{bmatrix} \tag{5}$$

where c_2, s_2 correspond to $\cos(q_2)$ and $\sin(q_2)$ respectively and c_{24}, s_{24} correspond to $\cos(q_2 + q_4)$ and $\sin(q_2 + q_4)$ respectively. The inertia tensor $\mathbf{I}$ and the friction terms for each joint have been identified in [6]. Thus by feed-forwarding the dynamics, the arm is compliant to user's arm motion, while adding the term $\mathbf{J}^T(\mathbf{q})\mathbf{F}$ the user has to exert force along the axes x, y in order to deform the virtual two-dimensional spring. Then, it is evident that the user exerts force to the environment (robot) which is equal in magnitude and opposite in the direction of the force $\mathbf{F}$. The Coriolis-Centrifugal forces of the robot are omitted as their contribution to the dynamic equation is minimal.

The processed EMG signals are recorded in the frequency of 1 kHz. For this reason, models outputs should be sampled at the same frequency. Regarding force exerted from the user to the environment (robot), it is acquired through the robot motor torque feedback measurements at the frequency of 500 Hz. Then they are resampled offline at the frequency of 1 kHz, using an anti-aliasing (lowpass) finite impulse response (FIR) filter. The user's joint angles are computed using the measurements of the two tracking sensors placed at points depicted in Fig. 1, as shown below:

$$q_s = \arctan 2(y_1, x_1), \quad q_e = \arctan 2\,(y_2 - y_1, x_2 - x_1) \tag{6}$$

where q_s, q_e the computed shoulder and elbow joint angles respectively and (x_1, y_1), (x_2, y_2) the coordinates of the sensors 1 and 2 respectively, with respect to the tracker reference system, as shown in Fig. 1. The frequency of the position tracker measurements is 60 Hz. Using the joint angles of the robot arm, and the kinematic equations (1), the position of the user's hand with respect to robot reference system can be calculated, as the user's hand is firmly coupled with the robotic end-effector. Having computed the relative position of the tracker reference system with respect to the robot base reference system at the start of the experimental procedure, user's hand position with respect to the tracker system can be calculated. By using these values, in conjunction with the low frequency tracker measurements, the user's joint angles can be reconstructed and sampled in the frequency of 500 Hz, offline. Afterwards, using an anti-aliasing FIR filter these measurements are sampled at the frequency of 1 kHz. The reason for not applying the filter at the original tracker measurements is the low acquisition frequency of the tracker (60 Hz) which would cause inaccurate joint angle values, especially in the cases of fast and jerky motions.

Therefore, EMG signals from 4 muscles (system inputs) as well as shoulder and elbow joint angles and exerted forces along x, y axes (system outputs) are available at the frequency of 1 kHz. The model relating the inputs with the outputs will be discussed in the following paragraphs.

A variety of models have been used for the utilization of EMG signals to control. A class of these models are based on human musculo-skeletal analysis (morphological models) while others consider the system as a black box [7]. Morphological modeling involves designing a model based on physical characteristics of the system. However, the large number of user-dependent parameters and the complexity of its equation, make this solution impractical. Therefore, the relationship between the EMG signal (input) and the joint motion and external force (output) will be obtained considering the system as a black box.

A linear time-invariant model is defined by

$$y(t) = G(z)\,u(t) + H(z)\,e(t) \tag{7}$$

where $u(t)$ the system input, $y(t)$ the system output, $e(t)$ white noise and $G(z)$, $H(z)$ polynomials of the backward shift operator z^{-1} of the form

$$G(z) = \sum_{k=1}^{\infty} g(k)\,z^{-k}, \qquad H(z) = 1 + \sum_{k=1}^{\infty} h(z)\,z^{-k} \tag{8}$$

In most cases, rational transfer functions and finite-dimensional state-space descriptors are used to specify G and H in terms of finite number of numerical values, or coefficients. Determination though of these coefficients has a most important consequence for the purpose of system identification [8]. Therefore these coefficients enter the model described by (7) as shown below:

$$y(t) = G(z,\theta)\,u(t) + H(z,\theta)\,e(t) \tag{9}$$

where the parameter vector θ ranges over a subset of $\mathbf{R}^d$, where d is the dimension of θ.

A set of models is defined by (9). It is for the estimation procedure to select a member in the set that appears to be the most suitable for the purpose in question. Variations in the form of G and H as given in (8) produce different kinds of linear time invariant models with specific intrinsic properties.

For the simplification of the identification algorithm, each of the four output variables of the model investigated will be estimated using a separate multi-input single-output linear time invariant model. Thus a family of four models, with four inputs and one output signal, will be identified at each case. Afterwards, the four identified models will constitute the final multi-input multi-output model. The estimation of the model parameters was implemented using the System Identification Toolbox in the software package Matlab™.

1) Auto-Regressive Moving Average with eXogenous output (ARMAX) model: An Auto-Regressive Moving Average with eXogenous output (ARMAX) model is given by (7), where G and H are given by:

$$G(z,\theta) = \frac{B(z,\theta)}{A(z,\theta)}, \qquad H(z,\theta) = \frac{C(z,\theta)}{A(z,\theta)} \tag{10}$$

where $A(z,\theta)$, $B(z,\theta)$, $C(z,\theta)$ are given by:

$$\begin{aligned} A(z,\theta) &= 1 + a_1 z^{-1} + \ldots + a_{n_a} z^{-n_a} \\ B(z,\theta) &= b_1 z^{-1} + \ldots + b_{n_b} z^{-n_b} \\ C(z,\theta) &= c_1 z^{-1} + \ldots + c_{n_c} z^{-n_c} \end{aligned} \tag{11}$$

where n_a, n_b, n_c the orders of the polynomials $A(z,\theta)$, $B(z,\theta)$ and $C(z,\theta)$ respectively. In the case of n_u inputs, the coefficients b_i are defined as $1 \times nu$ matrices. Therefore, for the case discussed, where four input signals are present, there are four polynomial functions given by:

$$B_i(z,\theta) = b_{i1} z^{-1} + \ldots + b_{in_{bi}} z^{-n_{bi}}, \quad i = 1,\ldots,4 \tag{12}$$

and the parameter vector to be identified is given by:

$$\theta = \begin{bmatrix} a_1 \ldots a_{n_a} & b_{11} \ldots b_{1n_{b_1}} & \ldots & b_{41} \ldots b_{4n_{b_4}} \end{bmatrix}^T \tag{13}$$

Four multiple-input single-output models of this form are constructed in order to relate muscle activity to the four desired variables. The criterion selected to compare model outputs with the corresponding measured values is defined by:

$$F_C = \sum_{k=1}^{4} 25 \left(1 - \frac{\left\| \hat{\mathbf{Y}}^{(k)} - \mathbf{y}^{(k)} \right\|}{\left\| \mathbf{y}^{(k)} - \bar{\mathbf{y}}^{(k)} \right\|} \right) \% \tag{14}$$

where $\hat{\mathbf{Y}}^{(\mathbf{k})}$ is the vector of size n containing the outputs from the model k at each time instance iT, where T the sampling period and $i = 1,\ldots,n$. $\mathbf{y}^{(k)}$ is the corresponding vector of the real measurements. The value of F_C tends to 100% as the accuracy of the model estimation increases. The order of each polynomial function B_i as well as the order of $A(z,\theta)\,y(t)$ and $C(z,\theta)\,y(t)$ is critical for achieving accurate estimation results. Orders from 1 to 10 are tested. The order of the B_1, B_2, B_3, B_4, C polynomials was the same: $n_{b1} = n_{b2} = n_{b3} = n_{b4} = n_{\mathbf{B}} = n_{\mathbf{C}}$. In Fig. 3a the fitting criterion is depicted for each of the possible combinations of n_a, $n_{\mathbf{B}}$. As it can be seen the maximum value of the criterion is 67% and was achieved for $n_a = 5$, $n_{\mathbf{B}} = n_C = 5$.

2) Output Error (OE) model: An Output Error (OE) model is given by (7), where G and H are given by:

$$G(z,\theta) = \frac{B(z,\theta)}{F(z,\theta)}, \quad H(q,\theta) = 1 \tag{15}$$

where $B(z,\theta)$ is defined as in (11) and $F(z,\theta)$ is given by

$$F(z,\theta) = 1 + f_1 z^{-1} + \ldots + f_{n_f} z^{-n_f} \tag{16}$$

where n_b, n_f the orders of the polynomials $B(z,\theta)$ and $F(z,\theta)$ respectively. In the case of n_u inputs, the coefficients b_i, f_i are defined as $1 \times nu$ matrices. Therefore, for the case discussed, where four input signals are present, B_i are given in (12), while F_i are given by:

$$F_i(z,\theta) = f_{i1} z^{-1} + \ldots + f_{in_{fi}} z^{-n_{fi}}, \quad i = 1,\ldots,4 \tag{17}$$

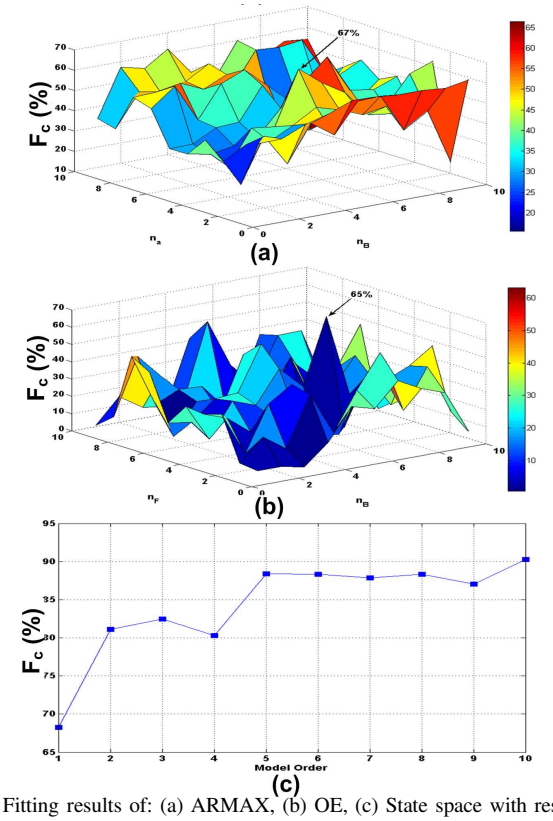

Fig. 3. Fitting results of: (a) ARMAX, (b) OE, (c) State space with respect to model orders.

The parameter vector to be estimated in this case is given by:

$$\begin{aligned} \theta = [&b_{11} \ldots b_{1n_{b_1}} \ldots \quad b_{41} \ldots b_{4n_{b_4}} \\ &f_{11} \ldots f_{1n_{f_1}} \ldots \quad f_{41} \ldots f_{4n_{f_4}}]^T \end{aligned} \tag{18}$$

The criterion used for comparing model estimates with measured values is the one defined in (14). Orders from one to ten were tested for each of the polynomials, while the order of the F_1, F_2, F_3, F_4 polynomials was the same: $n_{f1} = n_{f2} = n_{f3} = n_{f4} = n_{\mathbf{F}}$, while similar to the case of the ARMAX model: $n_{b1} = n_{b2} = n_{b3} = n_{b4} = n_{\mathbf{B}}$. In Fig. 3b the fitting criterion is depicted for each of the possible combinations of $n_{\mathbf{F}}$, $n_{\mathbf{B}}$. As it can be seen the maximum value of the criterion is 65% and was achieved for $n_{\mathbf{B}} = 6$, $n_{\mathbf{F}} = 4$.

3) State Space model: A linear time-invariant system can be described in discreet state space form by

$$\begin{aligned} \mathbf{x}((\mathbf{k}+\mathbf{1})\,\mathbf{T}) &= \mathbf{A}(\theta)\,\mathbf{x}(\mathbf{kT}) + \mathbf{B}(\theta)\,\mathbf{u}(\mathbf{kT}) \\ \mathbf{y}(\mathbf{kT}) &= \mathbf{C}(\theta)\,\mathbf{x}(\mathbf{kT}) \end{aligned} \tag{19}$$

where T the sampling period, $\mathbf{x}$ the state vector of size n, $\mathbf{u}$ the input vector of size n_u, $\mathbf{y}$ the output vector of size n_y, θ the vector of unknown parameters to be identified and $\mathbf{A}(\theta)$, $\mathbf{B}(\theta)$, $\mathbf{C}(\theta)$ matrices of size $n \times n$, $n \times n_u$ and $n_y \times n$ respectively.

In the case of four input signals and one output, matrices $\mathbf{A}(\theta)$, $\mathbf{B}(\theta)$ and $\mathbf{C}(\theta)$ are of size $n \times n$, $n \times 4$ and $1 \times n$ respectively, where n the order of the model and the length of the state vector $\mathbf{x}$. The criterion used for comparing model estimates with measured values is the one defined in (14). Model orders from one to ten were tested. In Fig. 3c the fitting criterion is depicted with respect to model order. As it can be seen the maximum value of the criterion is 90% and was achieved for the model of order $n = 10$.

Concerning the above cases, it must be noted that the fitting criterion is applied to experiments not used for the identification of each model. A state space model of order ten, was finally selected to be used for the estimation of motion and exerted force based on EMG signals, as it exhibits the best performance among the others. However, the accuracy of 90% in joint space, is not always satisfactory, especially when fine arm motions are considered. For this reason, during the operation of the system, low-frequency measurements of the position tracker are used in conjuction with the high-frequency EMG-based estimates of the state-space model, in order to output the final joint angles estimates. This is done by using a Kalman filter.

B. Filtering

If a state space model of order ten is selected for each of the desired outputs (i.e. shoulder and elbow joint angles, and x-y components of exerted force), then a total multi-input multi-ouput state space model can be defined as shown below:

$$\begin{aligned} \mathbf{x}\left((k+1)T\right) &= \mathbf{A_t}\mathbf{x}\left(kT\right) + \mathbf{B_t}\mathbf{u}\left(kT\right) \\ \mathbf{y}\left(kT\right) &= \mathbf{C_t}\mathbf{x}\left(kT\right) \end{aligned} \tag{20}$$

where $\mathbf{x} \in \Re^{40}$ the state vector, T the sampling period, $\mathbf{u} \in \Re^4$ the input vector, $\mathbf{y} \in \Re^4$ the output vector and matrices $\mathbf{A_t}, \mathbf{B_t}, \mathbf{C_t}$ given by:

$$\mathbf{A_t} = \begin{bmatrix} \mathbf{A_{S_1}} & \mathbf{0_{10}} & \mathbf{0_{10}} & \mathbf{0_{10}} \\ \mathbf{0_{10}} & \mathbf{A_{S_2}} & \mathbf{0_{10}} & \mathbf{0_{10}} \\ \mathbf{0_{10}} & \mathbf{0_{10}} & \mathbf{A_{S_3}} & \mathbf{0_{10}} \\ \mathbf{0_{10}} & \mathbf{0_{10}} & \mathbf{0_{10}} & \mathbf{A_{S_4}} \end{bmatrix}, \quad \mathbf{B_t} = \begin{bmatrix} \mathbf{B_{S_1}} \\ \mathbf{B_{S_2}} \\ \mathbf{B_{S_3}} \\ \mathbf{B_{S_4}} \end{bmatrix},$$
$$\mathbf{C_t} = \begin{bmatrix} \mathbf{C_{S_1}} & \mathbf{0_{1\times10}} & \mathbf{0_{1\times10}} & \mathbf{0_{1\times10}} \\ \mathbf{0_{1\times10}} & \mathbf{C_{S_2}} & \mathbf{0_{1\times10}} & \mathbf{0_{1\times10}} \\ \mathbf{0_{1\times10}} & \mathbf{0_{1\times10}} & \mathbf{C_{S_3}} & \mathbf{0_{1\times10}} \\ \mathbf{0_{1\times10}} & \mathbf{0_{1\times10}} & \mathbf{0_{1\times10}} & \mathbf{C_{S_4}} \end{bmatrix} \tag{21}$$

where $\mathbf{A_{S_i}}$, $\mathbf{B_{S_i}}$, $\mathbf{C_{S_i}}$, $i = 1, \ldots, 4$ matrices of size 10×10, 10×4, 1×10 respectively, identified for each of the signle-output state space models of the previous section, and $\mathbf{0_{10}}$, $\mathbf{0_{1\times10}}$ zero matrices of size 10×10 and 10×1 respectively. Matrices with subscript 1 correspond to identified model having as output the shoulder angle. Similarly subscripts 2, 3, 4 correspond to models having as outputs the elbow angle, the x and the y component of force respectively. For the application of the Kalman filter, the system is written as above:

$$\begin{aligned} \mathbf{x}\left((k+1)T\right) &= \mathbf{A_t}\mathbf{x}\left(kT\right) + \mathbf{B_t}\mathbf{u}\left(kT\right) + \mathbf{w}\left(kT\right) \\ \mathbf{z}\left(kT\right) &= \mathbf{H}\mathbf{x}\left(k\right) + v\left(kT\right) \end{aligned} \tag{22}$$

where $\mathbf{z}$ the measurement vector, $\mathbf{H}$ a 2×40 matrix relating measurement vector with the state vector $\mathbf{x} \in \Re^{40}$ while $\mathbf{w}$, v random variables representing the process and measurement noise respectively. The available measurements are the shoulder and elbow joint angles, through the position tracker measurements and eq. (6). Thus the $\mathbf{H}$ matrix that relates the state vector $\mathbf{x}$ to the measurement vector $\mathbf{z}$ is dependent only on $\mathbf{C_{S_1}}$, $\mathbf{C_{S_2}}$ and is defined by:

$$\mathbf{H} = \begin{bmatrix} \mathbf{C_{S_1}} & \mathbf{0_{1\times10}} & \mathbf{0_{1\times10}} & \mathbf{0_{1\times10}} \\ \mathbf{0_{1\times10}} & \mathbf{C_{S_2}} & \mathbf{0_{1\times10}} & \mathbf{0_{1\times10}} \end{bmatrix} \tag{23}$$

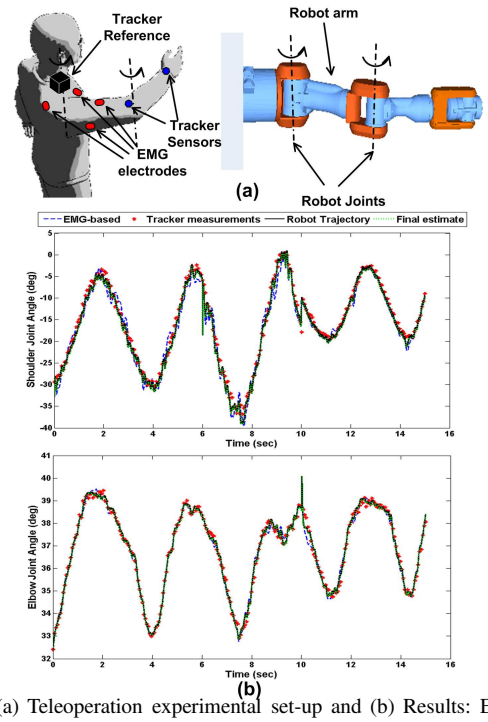

Fig. 4. (a) Teleoperation experimental set-up and (b) Results: EMG-based estimates, low-frequency tracker measurements and the Kalman filter form the final estimate for shoulder and elbow joint angle. The robot follows the commanded joint trajectory using the control law described in (25).

If $\hat{\mathbf{x}}\left(kT\right)$ the final estimate of the Kalman filter for the state vector, at time instance kT, then the output vector is given by:

$$\begin{aligned} \mathbf{y}\left(kT\right) &= \begin{bmatrix} q_s^f\left(kT\right) & q_e^f\left(kT\right) & F_{h_x}^f\left(kT\right) & F_{h_y}^f\left(kT\right) \end{bmatrix}^T \\ &= \mathbf{C_t}\hat{\mathbf{x}}\left(kT\right) \end{aligned} \tag{24}$$

where q_s^f, q_e^f, $F_{h_x}^f$, $F_{h_y}^f$ correspond to final estimates of shoulder and elbow joint angle, x and y components of force respectively. The architecture was tested in a variety of motions within different directions and velocity profiles.

III. Application to Teleoperation and Orthosis

A. Teleoperation Scenario

The teleoperation set-up used is shown in Fig. 4a. EMG signals are recorded from four muscles of the shoulder and elbow joint of the user, while position sensors are placed on the shoulder and elbow points as shown in Fig. 4a. The robot arm used is a 7-DoF manipulator (PA-10, Mitsubishi Heavy Industries). Two personal computers (PCs) in Linux environment were used: one PC communicates with the robot controller through ARCNET protocol in the frequency of 500 Hz, while the other PC acquires EMG signals and the position tracker measurements. The two PCs are connected through serial communication (RS-232) for synchronization purposes. The position tracking system used (Isotrak II, Polhemus Inc.) communicates with the PC through serial communication (RS-232).

During the real-time teleoperation, the estimates of motion and exerted force were used to control the robot arm, in terms of torque (i.e. sending torque commands to joint motors). For this reason, the control law applied is given by

$$\tau = \mathbf{I}\left(\ddot{\mathbf{q}} + \mathbf{K}_v\dot{\mathbf{e}} + \mathbf{K_p}\mathbf{e}\right) + \mathbf{F_{fr}}\left(\dot{\mathbf{q}}\right) + \mathbf{J^T}\left(\mathbf{q}\right)\mathbf{F_{ex}} \tag{25}$$

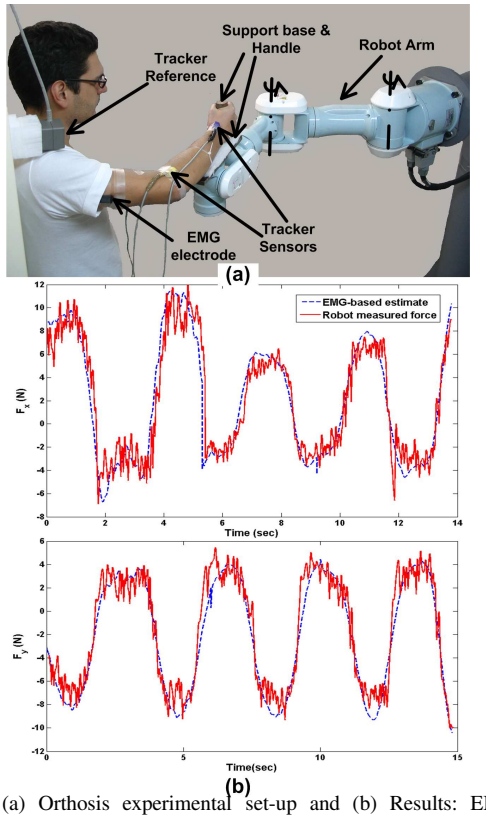

Fig. 5. (a) Orthosis experimental set-up and (b) Results: EMG-based estimates for x, y components of force fit to the corresponding force components computed from robot joint torque measurements.

where $\mathbf{F_{ex}} = \begin{bmatrix} F^f_{h_x} & F^f_{h_y} \end{bmatrix}^T$ the vector of exerted force, $\mathbf{K}_\upsilon$, $\mathbf{K_p}$ diagonal positive gain matrices of size 2×2 and $\mathbf{e}$ the joint angle error vector defined by:

$$\mathbf{e} = \begin{bmatrix} q^f_s - q_2 & q^f_e - q_4 \end{bmatrix}^T \tag{26}$$

where q_2, q_4, $\mathbf{I}$, $\mathbf{F_{fr}}$, $\mathbf{J}$ robot variables defined in (1), (4). Applying this control law, the robot joints are directed according to human shoulder and elbow joint angle estimates, while force is exerted through the robot end-effector equal to that estimated to being exerted from the human user. It must be noted that eq. (25) can be directly transformed to the corresponding discreet form, using as sampling frequency that of the robot (i.e. 500 Hz). Thus, an average of two EMG-based estimates of the output vector $\mathbf{y}$ are used for each robot control cycle, a characteristic that improves system accuracy and safety. In Fig. 4b, the performance of the system in joint space is depicted. As it can be seen, the EMG-based estimates for shoulder and elbow joint angles, in conjunction with the low-frequency measurements of the position tracker incorporated to the model through the Kalman filter, were able to control the robot arm with high accuracy. The system was tested in both slow and fast movements, exhibiting similar performance. The system performance in terms of user's force estimation is shown within the case of the orthosis.

B. Orthosis Scenario

In the case of the orthosis, the robot arm is coupled with the human arm, as shown in Fig. 5a. As it can be seen the user's arm motion is restricted to the plane, as the forearm and wrist are immobilized by means of straps that are coupled with the robot forearm, using a support base and a handle. Only two planar robotic joints are free to move, while the others are kept fixed in their initial position via electromechanical brakes. The user's arm is supported against gravitational forces. The user exert force through the handle, while moving his/her arm. This force is felt by the robot through the joint torque sensors, and can be computed using eq. (4), (5), by measuring the torque vector τ and the joint vector $\mathbf{q}$. The system performance is depicted in Fig. 5b, where the EMG-based estimates of force are compared with the corresponding force calculated from the torque measurements, along the x, y axes.

IV. Conclusion

This paper proposes a methodology of a combined position-force control of a robot arm using signals coming from both human muscles and artificial sensors. The human shoulder and elbow joint motion and the force exerted from the user to the environment are predicted using EMG signals from corresponding muscles and a position tracker, inputed to an identified state space model. The final estimates are used to control a torque-driven robot arm in the frequency of 500 Hz. Experiments conducted within two scenarios, including control of a remotely operated arm, as well as control of the arm coupled with the human upper limb, regarded as an orthosis. The accuracy of the system was proved high within a variety of motion profiles. The methodology can be applied to any teleoperated robot or orthotic device (exoskeleton), either for rehabilitation or extension of human ability, since the system is capable of providing accurate estimates of human motion and force.

ACKNOWLEDGMENTS

The authors want to acknowledge the contribution of the European Commission through contract NEUROBOTICS (FP6-IST-001917) project.

References

[1] O. Fukuda, T. Tsuji, A. Otsuka, and M. Kaneko, "Emg-based human-robot interface for rehabilitation aid," *Proc. of IEEE Int. Conf. on Robotics and Automation*, vol. 4, pp. 3492–3497, 1998.

[2] P. K. Artemiadis and K. J. Kyriakopoulos, "Emg-based teleoperation of a robot arm in planar catching movements using armax model and trajectory monitoring techniques," *Proc. of IEEE Int. Conf. on Robotics and Automation*, pp. 3244–3249, 2006.

[3] H. Kazerooni, "Human-robot interaction via the transfer of power and information signals," *IEEE Trans. Syst. Man, Cybern.*, vol. 20, no. 2, pp. 450–463, 1990.

[4] E. Cavallaro, J. Rosen, J. C. Perry, S. Burns, and B. Hannaford, "Hill-based model as a myoprocessor for a neural controlled powered exoskeleton arm- parameters optimization," *Proc. of IEEE Int. Conf. on Robotics and Automation*, pp. 4514–4519, 2005.

[5] J. Zhao, Z. Xie, L. Jiang, H. Cai, H. Liu, and G. Hirzinger, "Levenberg-marquardt based neural network control for a five-fingered prosthetic hand," *Proc. of IEEE Int. Conf. on Robotics and Automation*, pp. 4482–4487, 2005.

[6] N. A. Mpompos, P. K. Artemiadis, A. S. Oikonomopoulos, and K. J. Kyriakopoulos, "Modeling, full identification and control of the mitsubishi pa-10 robot arm," *IEEE/ASME International Conference on Advanced Intelligent Mechatronics, Switzerland, submitted*, 2007.

[7] D. T. Westwick, "Methods for the identification of multiple-input nonlinear systems," Ph.D. dissertation, Departments of Electrical Engineering and Biomedical Engineering, McGill University, Montreal, Quebec, Canada, 1995.

[8] L. Ljung, *System identification: Theory for the user*. Upper Saddle River, NJ: Prentice-Hall, 1999.